Hindawi Publishing Corporation
ISRN Electrochemistry
Volume 2014, Article ID 359019, 12 pages
http://dx.doi.org/10.1155/2014/359019

Research Article

Enhanced Structural Integrity and Electrochemical Performance of $AlPO_4$-Coated MoO_2 Anode Material for Lithium-Ion Batteries

José I. López-Pérez,[1,2,3] Edwin O. Ortiz-Quiles,[1,4] Khaled Habiba,[1,2] Mariel Jiménez-Rodríguez,[1,2,3] Brad R. Weiner,[1,3,4] and Gerardo Morell[1,2,3]

[1] *Institute of Functional Nanomaterials, University of Puerto Rico, Rio Piedras Campus, San Juan, PR 00931-3334, USA*
[2] *Department of Physics, University of Puerto Rico-Rio Piedras Campus, San Juan, PR 00936-8377, USA*
[3] *Center for Advanced Nanoscale Materials, University Research Center, University of Puerto Rico-Rio Piedras Campus, San Juan, PR 00931-3346, USA*
[4] *Department of Chemistry, University of Puerto Rico, Rio Piedras Campus, San Juan, PR 00931-3346, USA*

Correspondence should be addressed to José I. López-Pérez; lopez.joseismael@gmail.com

Received 24 December 2013; Accepted 15 January 2014; Published 4 March 2014

Academic Editors: S.-M. Lee and E. Vallés

$AlPO_4$ nanoparticles were synthesized via chemical deposition method and used for the surface modification of MoO_2 to improve its structural stability and electrochemical performance. Structure and surface morphology of pristine and $AlPO_4$-coated MoO_2 anode material were characterized by electron microscopy imaging (SEM and TEM) and X-ray diffraction (XRD). $AlPO_4$ nanoparticles were observed, covering the surface of MoO_2. Surface analyses show that the synthesized $AlPO_4$ is amorphous, and the surface modification with $AlPO_4$ does not result in a distortion of the lattice structure of MoO_2. The electrochemical properties of pristine and $AlPO_4$-coated MoO_2 were characterized in the voltage range of 0.01–2.5 V versus Li/Li^+. Cyclic voltammetry studies indicate that the improvement in electrochemical performance of the $AlPO_4$-coated anode material was attributed to the stabilization of the lattice structure during lithiation. Galvanostatic charge/discharge and electrochemical impedance spectroscopy (EIS) studies reveal that the $AlPO_4$ nanoparticle coating improves the rate capability and cycle stability and contributes toward decreasing surface layer and charge-transfer resistances. These results suggest that surface modification with $AlPO_4$ nanoparticles suppresses the elimination of oxygen vacancies in the lattice structure during cycling, leading to a better rate performance and cycle life.

1. Introduction

Lithium ion batteries are extensively used in a variety of portable electronic devices due to their high power density and long cycle life [1]. As reported, they are critically important for electric/hybrid vehicles as the power storage of the future [2]. Therefore, lithium ion batteries have attracted much interest in the field of fundamental study and applied research. Most commercialized lithium ion batteries use graphite as an anode material due to its accessibility and low cost; but its theoretical capacity is only 372 $mAh{\cdot}g^{-1}$ calculated by forming the compound of LiC_6 and cannot meet the ever-increasing demands for high capacity lithium ion technology [3]. By replacing graphite with transition metal oxides as anode materials, the capacity is enhanced. This is due to their close packed oxygen array, providing a framework structure and specific site for topotactic insertion and removal of lithium ions during charge/discharge process. A number of transition metal oxides have been studied and reported so far, including Mn_3O_4, Co_3O_4, MnO, TiO_2, NiO, MoO_2, and SnO_2, because of their possibility of various oxidation states and the search of new materials for energy storage [3, 4].

In order to improve structural stability and electrochemical behavior, many groups have demonstrated that the addition of a thin coating of metal phosphates, fluorides, oxides,

or other analogous materials onto the cathode particle results in reduced irreversible capacity, improved rate capability, and cycle life [5]. Surface modification of the electrode material by substitution is an effective method to improve the electrochemical properties [6]. Such substitutions are usually done for electrochemically active elements, causing lower capacity and Li^+ diffusion because the substitutions are usually electrochemically inactive ingredients. A coating approach is beneficial with respect to delivery of the initial capacity because there is no reduction of the amount of electrochemically active element in the electrode material. Therefore, a small amount of coating on the surface of electrode materials can improve the electrochemical properties [7–9]. The improvements in performance of these lithium ion cathodes by surface modification via the addition of coatings have been attributed to a diverse series of mechanisms, such as the coating promoting the retention of oxide ion vacancies in the crystal lattice after the first charge [10], suppression of the decomposition of the electrolyte [11], and the maintenance of low microstrain for better structural integrity and crystallinity during cycling [12].

Aluminum phosphate ($AlPO_4$), an environmentally friendly, lower cost, and thermally stable material, is of great interest in both environmental and technological fields [13]. With regard to the application of $AlPO_4$ for lithium ion batteries, other groups reported improvement concerning the safety and the electrochemical properties of the cathode materials by applying a direct coating of $AlPO_4$ nanoparticles from an aqueous solution [14–16]. Jiao et al. [17] successfully prepared $AlPO_4$-coated LiV_3O_8 powders by mixing active material LiV_3O_8 with $AlPO_4$ nanoparticle suspension followed by a low temperature heat treatment. The $AlPO_4$-coated material was found to reduce the capacity fading significantly. Manthiram and Wu [18] studied the effects of surface modification of Li_2MnO_3 and $LiMO_2$ (where M = Mn, Ni, and Co) solid solutions modified with 3 wt.% Al_2O_3, CeO_2, ZrO_2, SiO_2, ZnO, $AlPO_4$, and 0.05 atom F^- per formula unit and were characterized by XRD and charge/discharge measurements in lithium cells. Among all coating materials, results showed that the $AlPO_4$ modified sample had the largest reduction in irreversible capacity, compared to the rest of the samples modified with different coatings. Cho [19] reported that $LiCoO_2$ cathodes coated with $AlPO_4$ have improved their electrochemical performance due to the formation of homogeneous surface layers, in contrast with other coating materials (Al_2O_3 and ZrO_2).

Recently MoO_2, with a theoretical reversible capacity of ~838 $mAh{\cdot}g^{-1}$, has received much attention and has been considered as a promising anode material in lithium ion batteries because of its low electrical resistivity, high electrochemical activity, and high chemical stability [20]. One of the intrinsic drawbacks of MoO_2 for lithium ion battery applications is its volume expansion during Li^+ insertion/extraction process. The irreversible volume change causes MoO_2 particles to pulverize and crack, causing the detachment of the active material from the current collector, and consequently leading to a substantial loss in capacity [21]. In this context, we hereby present a study of the effects of $AlPO_4$ nanoparticle coating on the structural and electrochemical properties of MoO_2 anode material.

2. Experimental

Commercially available high purity chemicals were directly used without further purification. Pristine MoO_2 powder (Molybdenum (IV) oxide, Sigma Aldrich) was sintered at 350°C for 2 hours and ground thoroughly with an agate mortar and pestle, until a fine and homogeneous powder was obtained. To prepare $AlPO_4$-coated MoO_2, stoichiometric amounts of aluminum nitrate nonahydrate ($Al(NO_3)_3 9H_2O$-98%; Alfa Aesar) and ammonium hydrogen phosphate ($(NH_4)_2HPO_4$; Alfa Aesar) were dissolved separately in nanopure water. Ammonium hydrogen phosphate solution was slowly added to the aluminum nitrate nonahydrate solution until a white $AlPO_4$ nanoparticle suspension was observed. MoO_2 powder with an average particle size of ~5 μm was added to the coating solution and stirred thoroughly for 2 hours. The amount of $AlPO_4$ in the solution was ~3 wt.% of the MoO_2 powder. The solution was then filtered, dried at room temperature in air, and sintered at 400°C for 4 hours in flowing argon.

2.1. Electrode Preparation. Electrodes were prepared by spray coating Cu foil substrates with slurries of 90 wt.% anode powder, 5 wt.% carbon black (100% compressed, 99.5% metal basis; Alfa Aesar), and 5 wt.% PVDF binder (poly-vinylidene fluoride; Alfa Aesar) in 1-Methyl-2-pyrrolidinone (anhydrous, 99.5%; Sigma Aldrich). The pristine and $AlPO_4$-coated MoO_2 electrode materials were used as working electrodes. Coin cells were assembled inside an argon-filled glove box (M. Braun, USA) using stainless steel CR2032 coin cell hardware. Li metal foil was used as the counter and the reference electrode (0.75 mm thick × 19 mm wide, 99.9%, metal basis, Alfa Aesar). Electrodes inside the coin cell were separated using a Celgard 2400 membrane. Lithium hexafluorophosphate ($LiPF_6$) dissolved in a 1 : 1 molar ratio solution of dimethyl carbonate (DMC) and ethylene carbonate (EC) was used as the electrolyte. Multiple coin cells were assembled in order to validate the reproducibility of the surface analysis and electrochemical experiments.

2.2. Imaging and Surface Analysis Characterization. Powder X-ray diffraction (XRD) measurements were carried out using a Rigaku Ultima III X-ray diffractometer (Cu Kα radiation, Rigaku, Japan), at an accelerating potential of 40 kV and a tube current of 20 mA, to identify the crystalline phase of the synthesized pristine powders and $AlPO_4$-coated powders before and after lithiation. XRD data were collected at $3^\circ\,min^{-1}$ in the 2-theta range of 20–80°. Field emission scanning electron microscopy (FE-SEM, JSM-7500F, JEOL, Japan) was employed at working voltage of 15 kV to study the surface morphology of the prepared powders and cycled electrodes. Transmission electron microscopy (TEM, Carl Zeiss-LEO 922, Germany) at a working voltage of 200 kV and equipped with X-rays energy dispersive spectroscopy (XEDS) was used to determine the morphology and composition of

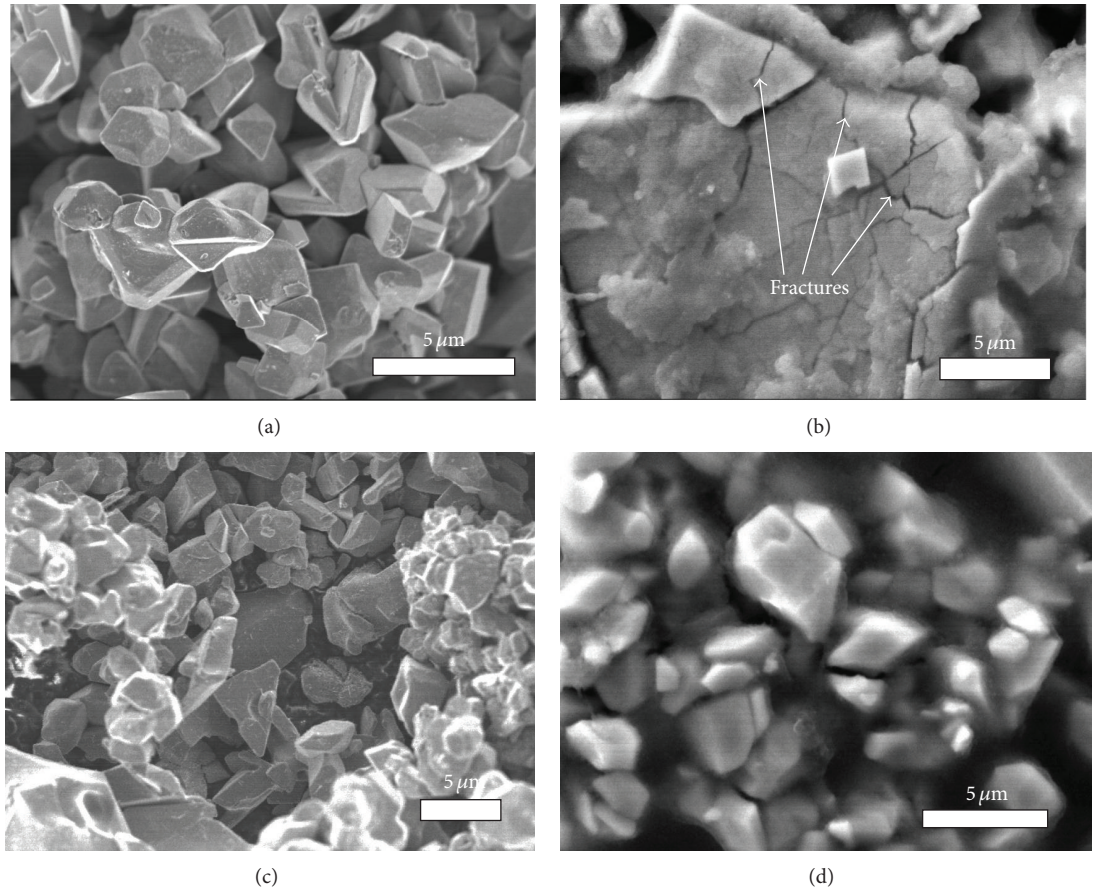

Figure 1: Scanning electron microscopy of pristine MoO_2 electrodes (a) before and (b) after cycling; and $AlPO_4$-coated MoO_2 electrodes (c) before and (d) after cycling.

the pristine and $AlPO_4$-coated samples. The samples were placed in a copper grid.

2.3. Electrochemical Characterization. Cyclic voltammetry (CV) tests were carried out at room temperature on a Series G-750 Potentiostat/Galvanostat/ZRA Gamry workstation in the potential window of 0.01–2.5 V versus Li/Li^+ at a scan rate of 0.2 mV s^{-1}. Galvanostatic charge and discharge capacity cycles were also carried out in this workstation at current densities of 50, 100, and 200 mA·g^{-1} between 0.01–2.5 V versus Li/Li^+ at room temperature. Electrochemical impedance spectroscopy (EIS) measurements were performed on a PARSTAT 2273 Potentiostat/Galvanostat (Advanced Measurement Tech. Inc.), with an applied AC signal amplitude of 5 mV peak-to-peak over a frequency range of 1 MHz to 10 mHz.

3. Results and Discussion

3.1. Imaging and Surface Analysis Characterization

3.1.1. Scanning Electron Microscopy (SEM). The morphology of the pristine and $AlPO_4$-coated MoO_2 electrodes, before and after cycling, is shown in Figure 1 in the scanning electron microscopy (SEM) images. Before cycling, the two powders were generally indistinguishable from one another. They have an average size of ~5 to 10 μm, indicating that the $AlPO_4$ coating did not lead to clumping or any other observable change in the microstructure of the anode particles. In comparison, cracks and crumbles are observed in the pristine material after cycling (Figure 1(c)) as a result of the large volume expansion during lithium insertion/extraction. This cracking and crumbling during cycling keeps generating new active surfaces that were previously passivated by the stable surface films [22]. Such cracks and crumbles are not observed (Figure 1(d)) in the $AlPO_4$-coated MoO_2 after cycling. It is quite likely that the $AlPO_4$ nanoparticle coating significantly reduces the formation of surface cracks induced by the volume expansion of the electrode material and therefore diminishes the repetitive formation of electrode/electrolyte interfaces affecting the capacity fading [22].

3.1.2. Transmission Electron Microscopy (TEM) and X-Ray Energy Dispersive Spectroscopy (XEDS). TEM images of pristine and $AlPO_4$-coated MoO_2 anode material were collected in order to determine the nature of the $AlPO_4$ coating nanoparticles. Figure 2(b) shows the core MoO_2 anode material uniformly covered by the $AlPO_4$ nanoparticles. Study

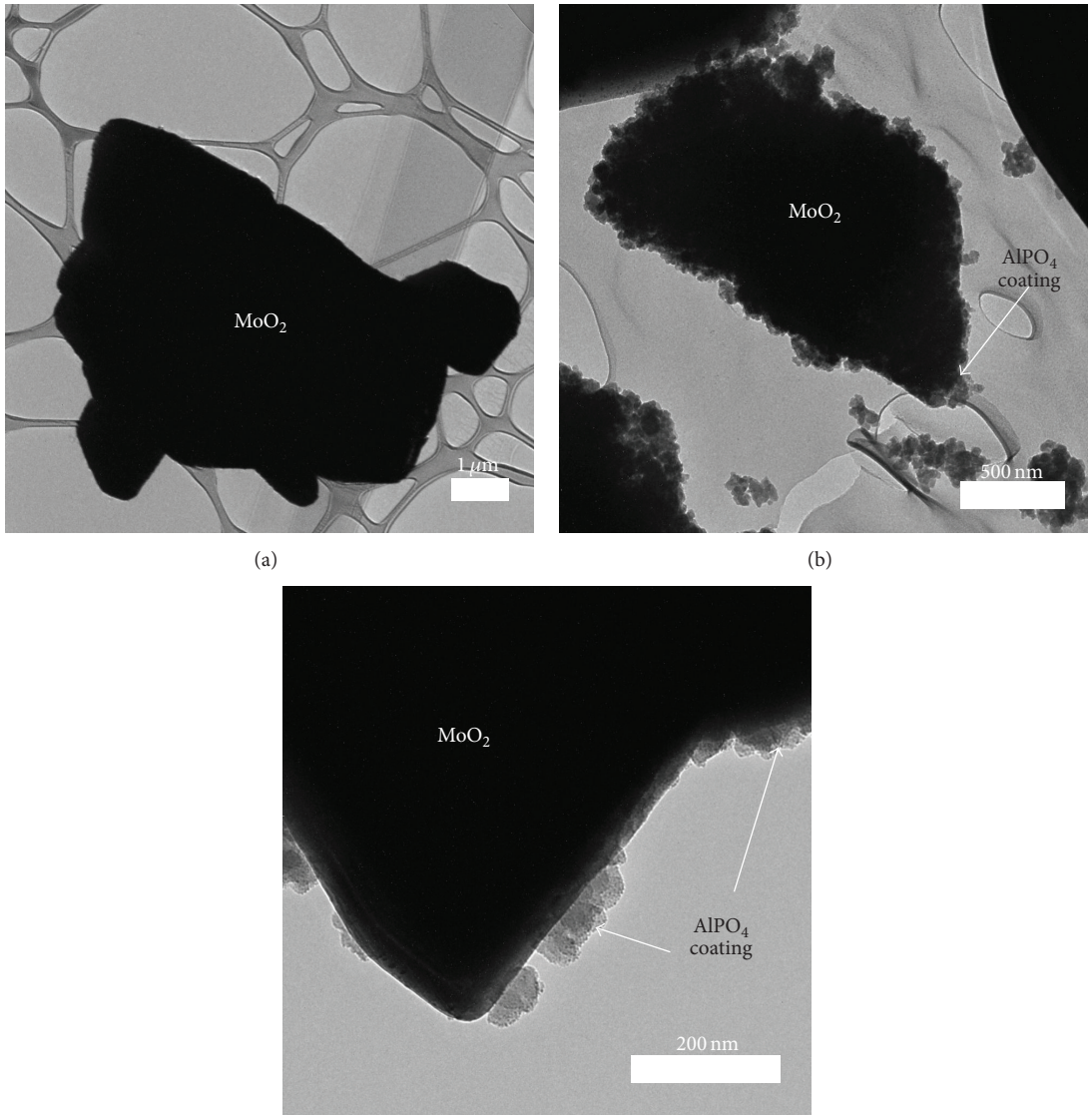

Figure 2: Transmission electron microscopy (TEM) images of (a) pristine MoO_2, (b) $AlPO_4$-coated MoO_2, and (c) $AlPO_4$ nanoparticle coating.

at higher magnification (Figure 2(c)) further reveals that the $AlPO_4$ nanoparticle coating consists of uniform particles with an average diameter of ~80 nm. The distribution of Al and P was examined by X-ray energy dispersive spectroscopy (XEDS) characterization technique and the results are displayed in Figure 3. EDS data confirm the presence of Al and P in the coating layer and the absence of Al or P components in the pristine sample. The presence of the Cu signal is due to the copper grid used in TEM analysis.

3.1.3. X-Ray Diffraction Analysis. The XRD patterns of pristine MoO_2 and $AlPO_4$-coated MoO_2 powders are shown in Figure 4. Figures 4(a) and 4(b) show the XRD patterns of the pristine and $AlPO_4$-coated MoO_2 powders before cycling, respectively. Both powders were confirmed to be well-defined monoclinic structure with the space group of $P2_{1/n}$, with no additional diffraction patterns related to $AlPO_4$ coating layer. Pristine and $AlPO_4$-coated powders showed the same lattice parameter values of $a = 5.606$ Å, $b = 4.859$ Å, and $c = 5.537$ Å (JCPDS card # 32-0671), revealing that the $AlPO_4$ coating was not incorporated into the anode material as no changes were perceived in the structure [23]. Furthermore, the two diffraction patterns overlap nearly identically, indicating that the sintering treatment or other procedures involved with the $AlPO_4$ coating did not result in distortion of the crystal lattice [5]. This result shows that the $AlPO_4$ is just coated on the surface of the MoO_2 powders [24]. Peaks between ~40–45° are characteristic of graphite [25], while the peaks at ~50° and ~74° correspond to the Cu-foil substrate (JCPDS card number 04-0836) [26]. As we want to evaluate if there are significant changes in

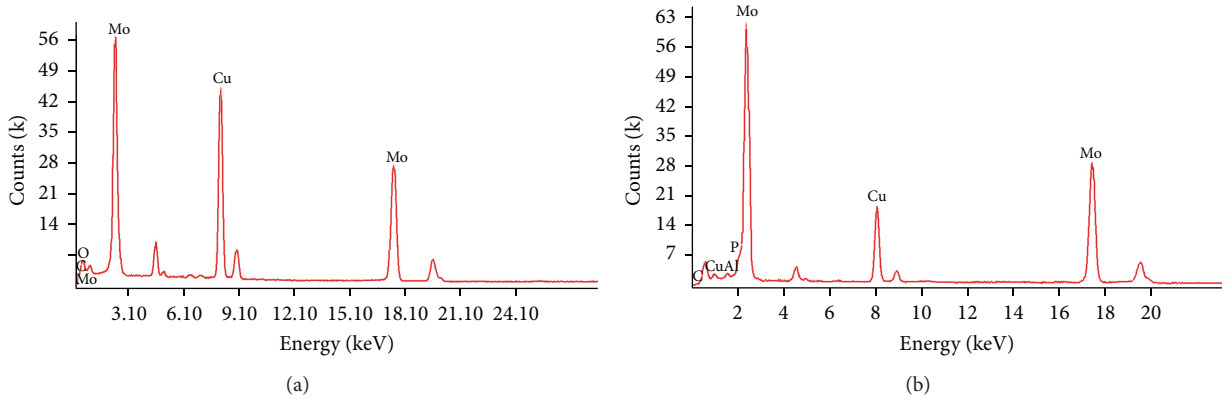

FIGURE 3: X-ray Electron Dispersion Spectroscopy (XEDS) data of (a) pristine MoO_2 and (b) $AlPO_4$-coated MoO_2 anode materials.

the lattice structure after cycling, lithium cells were opened inside and argon-filled glove box to recover the electrodes. These electrodes were rinsed in EC, dried under vacuum, and studied exposed by XRD. Figures 4(c) and 4(d) show the XRD data of the pristine and $AlPO_4$-coated MoO_2 samples after 50 cycles of galvanostatic charge and discharge. In the pristine sample (Figure 4(c)), a careful inspection reveals that diffraction peaks evolved in the 25°–35° 2theta range. This peak evolution, corresponding to Li_2O formation during lithiation process [27], may indicate a partial interchange of occupancy of Li^+ and transition metal ions, giving rise to disordering in the lattice structure due to an irreversible loss of oxygen during cycling [28]. This interchange of occupancy is known to deteriorate the electrochemical performance of the layered material [29, 30]. Such peaks are not observed in the $AlPO_4$-coated sample (Figure 4(d)). This probably suggests that the evenly dispersed $AlPO_4$ coating suppresses microstructural defects and structural degradation, acting as a protective coating layer, and therefore enhancing structural stability of MoO_2 electrode material.

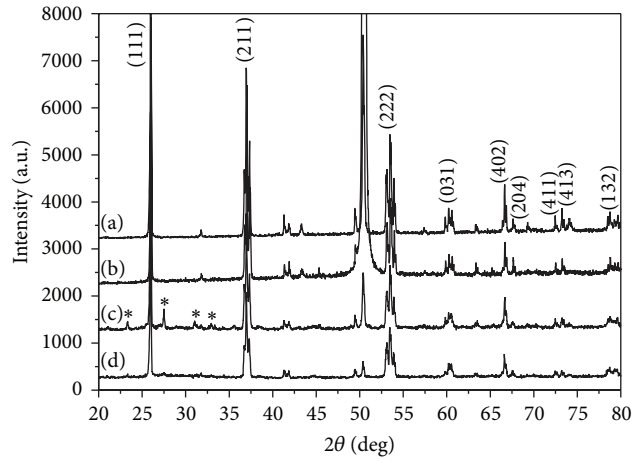

FIGURE 4: X-ray diffraction (XRD) patterns of (a) pristine MoO_2 and (b) $AlPO_4$-coated MoO_2 before cycling; and (c) pristine MoO_2 and (d) $AlPO_4$-coated MoO_2. Note the additional peaks of Li_2O (marked by asterisk) after 50 cycles of galvanostatic charge and discharge.

3.2. Electrochemical Characterization

3.2.1. Cyclic Voltammetry (CV) Studies. Cyclic voltammetry (CV) of pristine and $AlPO_4$-coated MoO_2 between 0.01–2.5 V at a scan rate of 0.2 mV s^{-1} was performed at room temperature to understand the effect of $AlPO_4$ coating on the Li^+ insertion/extraction behavior of MoO_2. Figure 5 shows two pairs of redox peaks at ~1.23/1.57 V versus Li/Li^+ and ~1.50/1.80 V versus Li/Li^+, corresponding to the reversible phase transition of Li_xMoO_2 and MoO_2 caused by the insertion and extraction of lithium ions [3, 31]. According to previous research [32, 33], the two reactions corresponding to the two redox processes observed in the cyclic voltammograms in Figure 5 are as follows:

$$MoO_2 + 4Li^+ + 4e^- \longrightarrow Mo + 2Li_2O \quad (1)$$

$$Mo + xLi^+ + xe^- \longleftrightarrow Li_xMoO_2 \quad (2)$$

During discharge, the lithium bonds to the oxygen in MoO_2, forming Mo metal and Li_2O. Then, the Mo partially alloys/dealloys up to the theoretical limit of Li_xMoO_2 (~838 mAh·g^{-1}). For pristine MoO_2 (Figure 5(a)), oxidation peaks slightly shift to higher potentials while the reduction peaks slightly shift to lower potentials (indicated with arrows). In addition, as cycling proceeds, oxidation and reduction peak intensities decrease rapidly. This electrochemical behavior indicates the structural degradation of MoO_2 anode material and an increase in the internal resistance during cycling, leading to the fast capacity loss of the pristine MoO_2 anode material [24, 34]. Electrodes suffer from capacity loss and poor rate capability because there are incomplete reversible phase transition and local structural damages during lithiation. On the other hand, it is observed that the $AlPO_4$-coated MoO_2 (Figure 5(b)) shows better cycling stability compared to pristine MoO_2. During cycling, almost no oxidation and reduction peak shifts are observed, suggesting a more stable lattice structure. Furthermore, the peak intensity declines much slower than that of the pristine MoO_2, indicating that capacity retention is noticeably enhanced after the $AlPO_4$ nanoparticle coating.

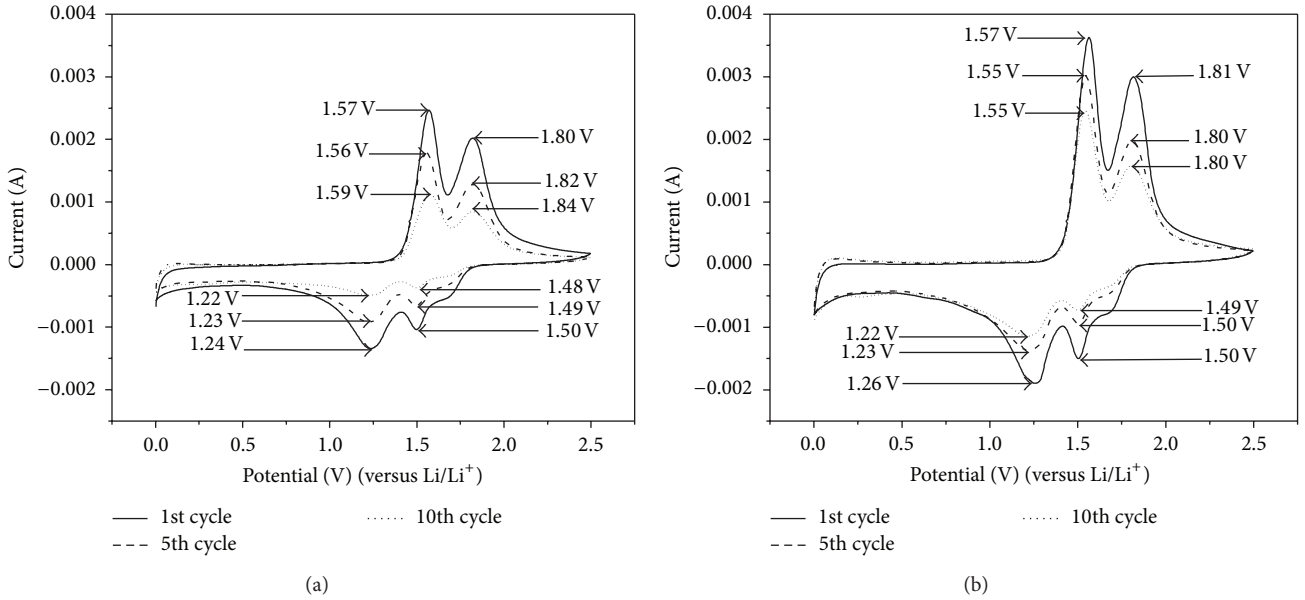

FIGURE 5: Cyclic voltammetry (CV) of (a) pristine MoO_2 and (b) $AlPO_4$-coated MoO_2 in the potential window of 0.01–2.5 V versus Li/Li^+ at a scan rate of 0.2 mV s^{-1} with 1 : 1 molar solution of $LiPF_6$ as electrolyte.

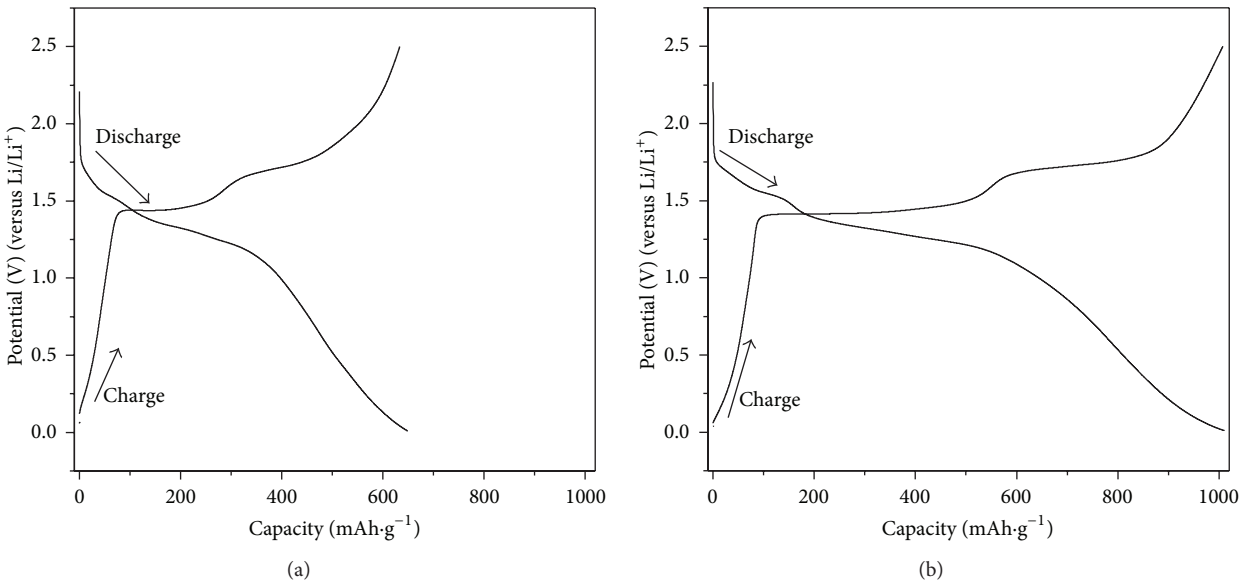

FIGURE 6: Initial charge/discharge curves of (a) pristine MoO_2 and (b) $AlPO_4$-coated MoO_2 anode material at a current density of 50 mA·g^{-1} in the voltage range of 0.01–2.5 V versus Li/Li^+.

3.2.2. Galvanostatic Charge and Discharge Capacity Studies. To study the electrochemical performance of pristine and $AlPO_4$-coated MoO_2, charge and discharge capacities were measured at a potential window of 0.01–2.5 V at current densities of 50, 100, and 200 mA·g^{-1} at room temperature. The first charge and discharge cycles for pristine and $AlPO_4$-coated MoO_2 electrodes, at a constant current density of 50 mA·g^{-1}, are represented in Figure 6. The first cycle charge capacity has been observed to be higher in the case of the $AlPO_4$-coated anode material (~1008 mAh·g^{-1}) compared to the pristine anode material (~625 mAh·g^{-1}). On the other hand, a higher first cycle discharge capacity is observed in the case of $AlPO_4$-coated MoO_2 (~1015 mAh·g^{-1}) compared to the pristine MoO_2 (~650 mAh·g^{-1}). These enhanced first cycle charge and discharge capacities can be attributed to the effective removal of lithium and oxygen from the host structure [35]. In both samples, there are two constant potential plateaus at ~1.40 and 1.70 V on the first

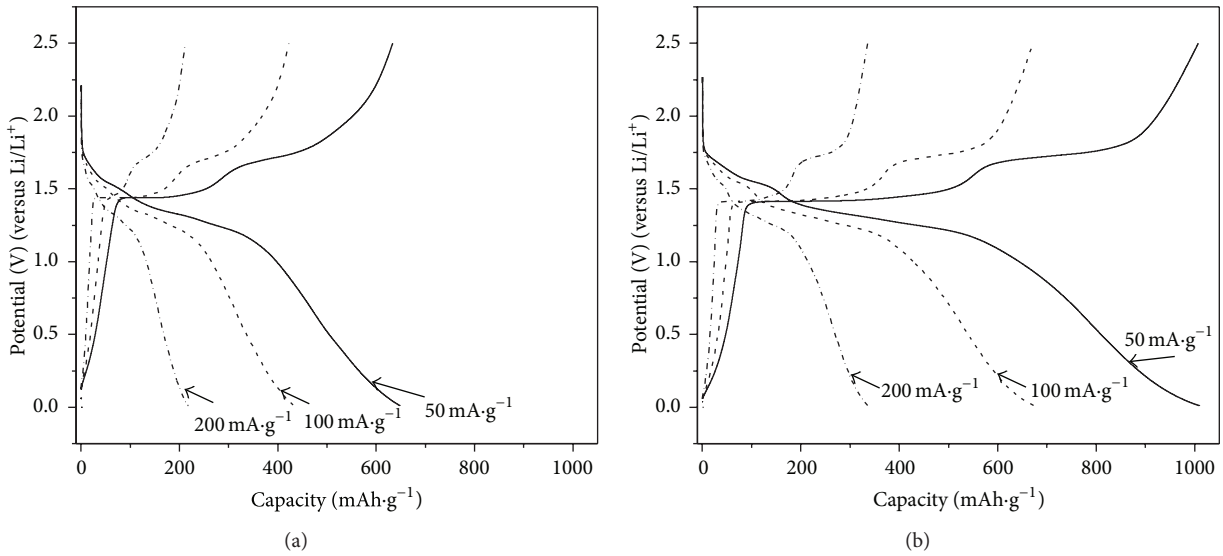

FIGURE 7: Initial charge and discharge curves of (a) pristine MoO_2 and (b) $AlPO_4$-coated MoO_2 at current densities of 50, 100, and 200 $mA{\cdot}g^{-1}$ between 0.01–2.5 V versus Li/Li^+ at room temperature.

charge cycles, as well as two potential plateaus at ~1.57 and 1.3 V on the first discharge cycles. These results are consistent with those reported by Liang et al. [33], since the inflection points between these potential plateaus represent a transition between monoclinic phase and orthogonal phase in the partially Li_xMoO_2. It is clearly observed that surface modification with $AlPO_4$ nanoparticles can significantly improve the electrochemical performance of MoO_2 anode material. Pristine MoO_2 electrode shows an irreversible capacity (IRC) of 25 $mAh{\cdot}g^{-1}$ during the first cycle, while the $AlPO_4$-coated MoO_2 electrode shows an irreversible capacity of 7 $mAh{\cdot}g^{-1}$ during the first cycle. The observed IRC and initial discharge capacity values confirm that oxide ion vacancies are partially retained in the lattice during the initial charge. In other words, we can imply that surface modification suppresses the elimination of oxide ion vacancies. This could be attributed to the mechanism proposed by Armstrong et al. [36], suggesting that surface modification suppresses the elimination of oxygen vacancies during the initial charge and consequently allows a reversible insertion/extraction of higher amounts of lithium in the subsequent discharge cycles [36]. Figure 7 shows the initial charge and discharge profiles of the pristine and $AlPO_4$-coated MoO_2 anode materials at current densities of 50, 100, and 200 $mA{\cdot}g^{-1}$. As shown in Figure 7(a), the initial discharge capacity of the pristine MoO_2 is 434 $mAh{\cdot}g^{-1}$ at a current density of 100 $mA{\cdot}g^{-1}$. When the current density is increased to 200 $mA{\cdot}g^{-1}$, pristine MoO_2 only undergoes an initial discharge capacity of 219 $mAh{\cdot}g^{-1}$. The pristine MoO_2 exhibits a relatively poor rate capability. Comparatively, the $AlPO_4$-coated MoO_2 exhibits an enhanced rate capability as illustrated in Figure 7(b). The discharge capacities of the $AlPO_4$-coated MoO_2 at current densities of 100 and 200 $mA{\cdot}g^{-1}$ are 647 and 341 $mAh{\cdot}g^{-1}$, respectively, indicating that the $AlPO_4$ nanoparticle coating significantly improves rate capability. The electrochemical data collected from the pristine and $AlPO_4$-coated MoO_2 electrodes are denoted in Table 1.

Now, let us compare the cycle performance of pristine and $AlPO_4$-coated MoO_2 electrodes considering the discharge capacity as a function of cycle number for the first 50 cycles, as presented in Figure 8. At a current density of 50 $mA{\cdot}g^{-1}$, pristine MoO_2 exhibits an initial discharge capacity of 650 $mAh{\cdot}g^{-1}$, as discussed above. It declines to 297 $mAh{\cdot}g^{-1}$ after 50 cycles, with a capacity loss of 54%. By contrast, the $AlPO_4$-coated MoO_2 electrode delivers an initial discharge capacity of 1015 $mAh{\cdot}g^{-1}$. It declines to 787 $mAh{\cdot}g^{-1}$ after 50 cycles, with a capacity loss of 22%. Rate capability, cycling stability, and discharge capacities of the $AlPO_4$-coated samples are improved after 50 cycles compared to the pristine samples. However, with ongoing cycling, lithium ions can eventually penetrate the coating protective layer, thus becoming incorporated into the lattice of MoO_2. This can be ascribed to the gradual elimination of oxygen vacancies in the anode material, which can be part of the reason for the capacity fading during cycling. Generally, this improvement in the discharge capacity, rate capability, and cycling stability can be explained due to the obstruction of the transition metal ions by the $AlPO_4$ nanoparticle coating to migrate from the surface to the bulk in the vacant sites for the lithium insertion, therefore maintaining the high concentration of the available sites for lithium insertion [10]. The $AlPO_4$ coating is an electronic insulator, as reported by Kim et al. [22], indicating that most of the oxidation and reduction reactions with lithium ions and electrons occur mainly at the interface between the anode material and $AlPO_4$ coating and not at the interface of $AlPO_4$ coating and electrolyte. From these results, we conclude that $AlPO_4$-coated anode material holds better cycling performance compared to the pristine anode material.

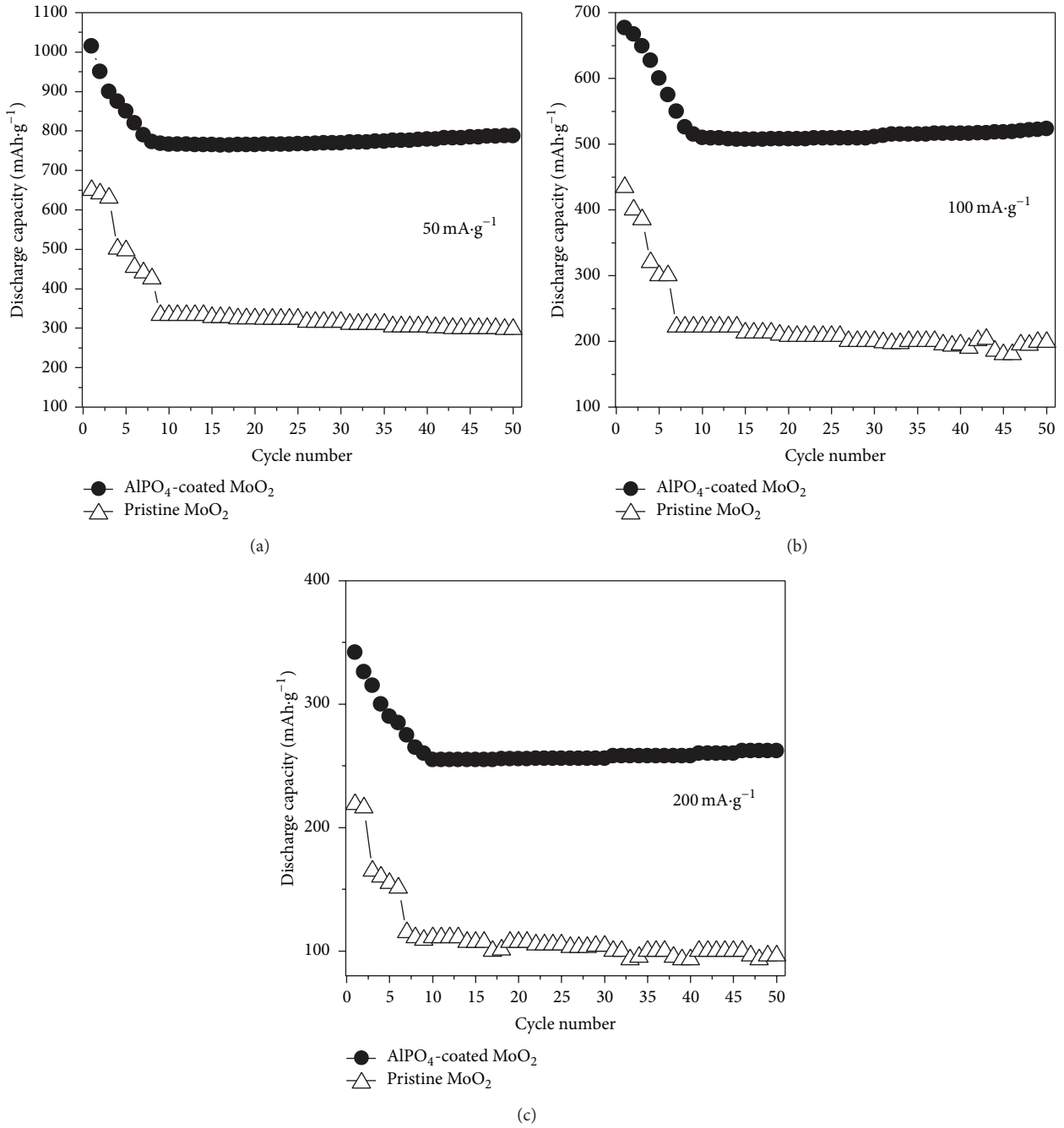

Figure 8: Discharge capacity as a function of cycle number of pristine MoO_2 and $AlPO_4$-coated MoO_2.

Table 1: Electrochemical data of galvanostatic charge and discharge cycles for pristine and $AlPO_4$-coated MoO_2.

Current density (mA g^{-1})	Pristine MoO_2				$AlPO_4$-coated MoO_2			
	Initial discharge capacity (mAh g^{-1})	Initial charge capacity (mAh g^{-1})	IRC (mAh g^{-1})	% Capacity loss after 50 cycles	Initial discharge capacity (mAh g^{-1})	Initial charge capacity (mAh g^{-1})	IRC (mAh g^{-1})	% Capacity loss after 50 cycles
50	650	625	25	54	1015	1008	7	22
100	434	413	21	—	677	673	4	—
200	201	201	18	56	341	338	3	24

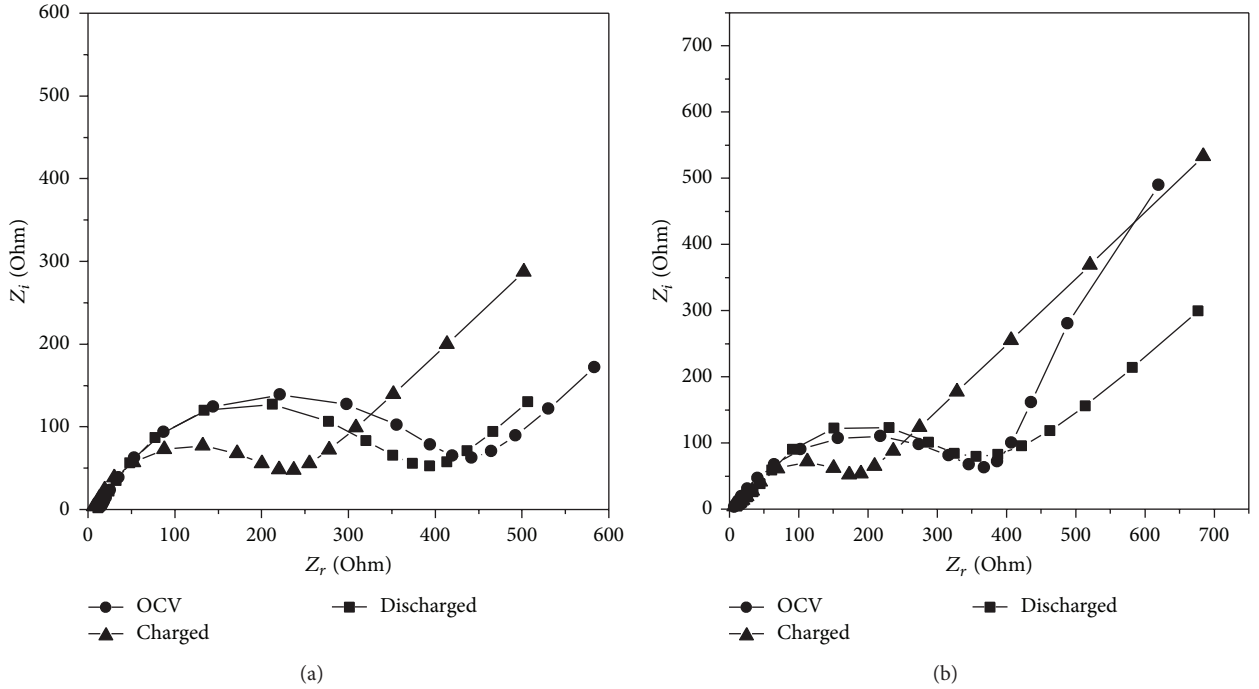

Figure 9: Electrochemical impedance spectroscopy (EIS) data of (a) pristine MoO_2 and (b) $AlPO_4$-coated MoO_2 with an applied AC signal amplitude of 5 mV peak-to-peak over a frequency range of 1 MHz to 10 mHz. EIS data were obtained after 3 cycles of galvanostatic charge and discharge at room temperature.

3.2.3. Electrochemical Impedance Spectroscopy (EIS). To better understand the reason for the enhanced electrochemical properties of the $AlPO_4$ nanoparticle coating, electrochemical impedance spectroscopy (EIS) was carried out for the pristine and $AlPO_4$-coated MoO_2 anode materials. The electrochemical impedance data were obtained after 3 cycles of galvanostatic charge and discharge at room temperature, since the solid electrolyte interface (SEI) film is formed during the first few cycles and changes very little during ongoing cycling [37]. EIS is an effective, nondestructive technique to understand the various phenomena occurring at the interface between the electrode and electrolyte. It is used to determine electrochemical cell impedance in response to a small AC signal at constant DC voltage over a broad frequency range, from MHz to mHz [38]. Impedance spectroscopy is a crucial parameter to determine the electrochemical performance of lithium ion batteries. With this characterization technique, different electrochemical processes occurring inside lithium ion batteries, such as charge transfer, double layer capacitance, and diffusion of ions in the electrode, can be studied by calculating the real and imaginary parts of the impedance. EIS measurements have been carried out on the lithium ion batteries to examine the electrochemical systems, involving interfacial processes and kinetics of electrode reactions, for the pristine MoO_2 and the $AlPO_4$-coated MoO_2. The results are shown in Figures 9(a) and 9(b), respectively, in the form of Nyquist plots. Determining the possible equivalent circuit, in order to interpret the data, is crucial in this electrochemical characterization technique [39]. The equivalent circuit used for fitting the impedance data is shown in Figure 10. From

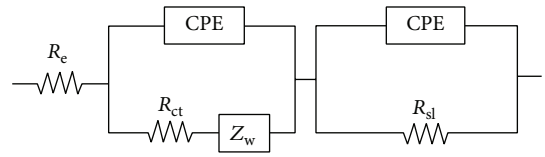

Figure 10: Equivalent circuit model for the EIS, where CPE are the constant phase elements, R_e—electrolyte resistance, R_{sl}—surface layer resistance, R_{ct}—charge transfer resistance, and Z_w—Warburg impedance.

the Nyquist plots, it can be perceived that they are composed of two parts. The first one is a suppressed semicircle in the high-middle frequency region related to charge-transfer process, and the second one is an oblique straight line in the low frequency region representing typical Warburg impedance.

The suppression of the semicircle in the Nyquist plots is due to the overlap of two different semicircles. The appearance of two suppressed semicircles indicates the contribution of two different resistive elements to the total impedance of the electrochemical cell. This is observed generally in the impedance plot due to the combination of a capacitor element and a resistor element in parallel. The semicircle in the high frequency region corresponds to the resistance (R_{sl}) due to the surface layer, or solid electrolyte interface (SEI) formation [40]. Capacity fading of the anode material during cycling is associated with the thickness of such layer on the anode particles. During cycling, the SEI layer grows thick due

Table 2: Electrochemical impedance spectroscopy (EIS) data parameters obtained after fitting, based on the model shown in Figure 10.

Fitted parameters	Pristine MoO_2			$AlPO_4$-coated MoO_2		
	OCV	Charged	Discharged	OCV	Charged	Discharged
R_e (Ohm)	15.9	7.49	13.2	7.74	7.24	12.81
R_{ct} (Ohm)	313.6	167.9	288.7	244	123.6	271.7
R_{sl} (Ohm)	38.07	21.81	34.62	24.57	15.78	28.37

to the electrode/electrolyte reaction, thus deteriorating the electrochemical performance of the cell. Middle frequency semicircle corresponds to the charge transfer resistance (R_{ct}) across the interface and the low frequency oblique straight line arises due to the lithium ion diffusion in the bulk of the anode material [41]. The intercept value on the x-axis in the high frequency region corresponds to the resistance (R_e) due to the lithium ion conduction in the electrolyte [41]. Depression in the semicircle has been calculated by placing constant phase elements (CPEs) instead of pure capacitance, as shown in the equivalent circuit. Impedance parameters obtained after fitting the EIS experimental data are summarized in Table 2.

By analyzing the data we observed that the main influence to the impedance is from the charge transfer resistance (R_{ct}) and surface layer resistance (R_{sl}). R_e behavior has been observed to be similar in both samples. In the charged state, it is observed that the R_{ct} value for the $AlPO_4$-coated MoO_2 is lower compared to that of the pristine MoO_2, and an increase in R_{sl} is observed, respectively. This increase in the value of R_{sl} is expected, due to the growth of the SEI layer at the electrode/electrolyte interface. In the case of the $AlPO_4$-coated sample, the decrease in the R_{ct} value can be explained due to the fact that, during cycling, irreversible extraction of the oxygen and lithium occurs, creating vacancies in the crystal structure of the anode material and, therefore, leading to the decrease in the charge transfer resistance [42]. The decrease in R_{ct} is helpful for improving the electron kinetics of the anode material, and, hence, enhancing the electrochemical performance of MoO_2 as anode material for lithium ion batteries [43]. On the other hand, in the discharged state, we observed that both R_{ct} and R_{sl} from the $AlPO_4$-coated sample are relatively low compared to the pristine sample. Charge transfer process is considered to be a rate determining process, and the rate performance of the anode material particularly depends on the R_{ct} [40]. $AlPO_4$ nanoparticle coating can support reducing the increase in charge transfer resistance, and, therefore, implying a better rate performance, compared to the pristine sample. These results are consistent with previous studies, indicating that charge transfer resistance decreases significantly with the incorporation of coatings [41, 44].

4. Conclusions

MoO_2 anode material has been successfully coated by $AlPO_4$ nanoparticles and the $AlPO_4$-coated electrode displays an enhancement in cycle-life performance. The $AlPO_4$ coating significantly reduces the formation of surface cracks induced by the volume expansion of MoO_2 anode material, diminishing the repetitive formation of electrode/electrolyte interfaces that affects the capacity fading. Electrochemical performance of pristine and $AlPO_4$-coated MoO_2 has been studied by galvanostatic charge and discharge, cyclic voltammetry (CV), and electrochemical impedance spectroscopy (EIS), in the voltage range of 0.01–2.5 V, indicating that the $AlPO_4$-coated MoO_2 exhibits enhanced rate capability and excellent cycle stability. Galvanostatic charge and discharge measurements, at a current density of 50 $mA{\cdot}g^{-1}$, reveal that pristine MoO_2 exhibits an initial discharge capacity of 650 $mAh{\cdot}g^{-1}$ and 54% capacity loss in 50 cycles, while the $AlPO_4$-coated MoO_2 exhibits an initial discharge capacity of 1015 $mAh{\cdot}g^{-1}$ and only 22% capacity loss at 50 cycles. Cyclic voltammetry studies indicate that the improvement in cycling performance of the $AlPO_4$-coated MoO_2 that is attributed to the stabilization of the lattice structure due to the suppression of the elimination of oxygen vacancies from the anode material. Electrochemical impedance spectroscopy (EIS) shows that the $AlPO_4$ nanoparticle coating reduces the surface layer and charge transfer resistance. Surface modification with $AlPO_4$ nanoparticles is an effective way to improve the structural stability and electrochemical performance of MoO_2 as anode material for lithium ion batteries.

Conflict of Interests

The authors declare that there is no conflict of interests regarding the publication of this paper.

Acknowledgments

This research project was carried out under the auspices of the Institute for Functional Nanomaterials (NSF Grant no. 1002410). This research was also supported in part by NSF GK-12 (NSF Grant no. 0841338), PR NASA EPSCoR (NNX13AB22A), PR NASA Space Grant (NNX10AM80H), and NASA Center for Advanced Nanoscale Materials (NNX08BA48A). The authors gratefully acknowledge the instrumentation and technical support of the Nanoscopy Facility (Dr. M. Guinel), the XRD and Glovebox Facilities (Dr. R. S. Katiyar), and helpful discussions with Dr. Vladimir Makarov.

References

[1] B. Scrosati, "Recent advances in lithium ion battery materials," *Electrochimica Acta*, vol. 45, no. 15-16, pp. 2461–2466, 2000.

[2] B. Kang and G. Ceder, "Battery materials for ultrafast charging and discharging," *Nature*, vol. 458, no. 7235, pp. 190–193, 2009.

[3] Q. Tang, Z. Shan, L. Wang, and X. Qin, "MoO_2-graphene nanocomposite as anode material for lithium-ion batteries," *Electrochimica Acta*, vol. 79, pp. 148–153, 2012.

[4] V. Pralong, "Lithium intercalation into transition metal oxides: a route to generate new ordered rock salt type structure," *Progress in Solid State Chemistry*, vol. 37, no. 4, pp. 262–277, 2009.

[5] W. C. West, J. Soler, M. C. Smart et al., "Electrochemical behavior of layered solid solution Li_2MnO_3-$LiMO_2$ (M Ni, Mn, Co) li-ion cathodes with and without alumina coatings," *Journal of the Electrochemical Society*, vol. 158, no. 8, pp. A883–A889, 2011.

[6] J. Sun, X. Ma, C. Wang, and X. Han, "Effect of $AlPO_4$ coating on the electrochemical properties of $LiNi_{0.8}Co_{0.2}O_2$ cathode material," *Journal of Alloys and Compounds*, vol. 453, no. 1-2, pp. 352–355, 2008.

[7] S. T. Myung and K. Izumi, "Role of alumina coating on Li–Ni–Co–Mn–O particles as positive electrode material for lithium-ion batteries," *Chemistry of Materials*, vol. 17, pp. 3695–3704, 2005.

[8] A. M. Kannan, L. Rabenberg, and A. Manthiram, "High capacity surface-modified $LiCoO_2$ cathodes for lithium-ion batteries," *Electrochemical and Solid-State Letters*, vol. 6, no. 1, pp. A16–A18, 2003.

[9] H. Cao, B. J. Xia, Y. Zhang, and N. X. Xu, "$LiAlO_2$-coated $LiCoO_2$ as cathode material for lithium ion batteries," *Solid State Ionics*, vol. 176, no. 9-10, pp. 911–914, 2005.

[10] Y. Wu and A. Manthiram, "Effect of surface modifications on the layered solid solution cathodes (1-z) $Li[Li_{1/3}Mn_{2/3}]O_2-$ (z) $Li[Mn_{0.5-y}Ni_{0.5-y}Co_{2y}]O_2$," *Solid State Ion*, vol. 180, pp. 50–56, 2009.

[11] J. Ying, C. Wan, and C. Jiang, "Surface treatment of $LiNi_{0.8}Co_{0.2}O_2$ cathode material for lithium secondary batteries," *Journal of Power Sources*, vol. 102, no. 1-2, pp. 162–166, 2001.

[12] A. M. Kannan and A. Manthiram, "Surface/chemically modified $LiMn_2O_4$ cathodes for lithium-ion batteries," *Electrochemical and Solid-State Letters*, vol. 5, no. 7, pp. A167–A169, 2002.

[13] B. Hu, X. Wang, Y. Wang et al., "Effects of amorphous $AlPO_4$ coating on the electrochemical performance of BiF_3 cathode materials for lithium-ion batteries," *Power Sources*, vol. 218, pp. 204–211, 2012.

[14] J. Cho, Y.-W. Kim, B. Kim, J.-G. Lee, and B. Park, "A breakthrough in the safety of lithium secondary batteries by coating the cathode material with AIPO4 nanoparticles," *Angewandte Chemie (International Edition)*, vol. 42, no. 14, pp. 1618–1621, 2003.

[15] K. S. Tan, M. V. Reddy, G. V. S. Rao, and B. V. R. Chowardi, "Effect of $AlPO_4$-coating on cathodic behaviour of $Li(Ni_{0.8}Co_{0.2})O_2$," *Journal of Power Sources*, vol. 141, pp. 129–142, 2005.

[16] J. Y. Shi, C.-W. Yi, and K. Kim, "Improved electrochemical performance of $AlPO_4$-coated $LiMn_{1.5}Ni_{0.5}O_4$ electrode for lithium-ion batteries," *Journal of Power Sources*, vol. 195, no. 19, pp. 6860–6866, 2010.

[17] L. F. Jiao, L. Liu, J. L. Sun et al., "Effect of $AlPO_4$ nanowire coating on the electrochemical properties of LiV_3O_8 cathode material," *Journal of Physical Chemistry C*, vol. 112, no. 46, pp. 18249–18254, 2008.

[18] A. Manthiram and Y. Wu, "Effect of surface modifications on the layered solid solution cathodes (1-z) $Li[Li_{1/3}Mn_{2/3}]O_2$-(z) $Li[Mn_{0.5-y}\ Ni_{0.5-y}\ Co_{2y}]O_2$," *Solid State Ion*, vol. 180, pp. 50–56, 2009.

[19] J. Cho, "Correlation between $AlPO_4$ nanoparticle coating thickness on $LiCoO_2$ cathode and thermal stability," *Electrochimica Acta*, vol. 48, no. 19, pp. 2807–2811, 2003.

[20] Y. M. Sun, X. L. Hu, W. Luo, and Y. H. Huang, "Self-assembled hierarchical MoO_2/graphene nanoarchitectures and their application as a high-performance anode material for lithium-ion batteries," *ACS Nano*, vol. 5, no. 9, pp. 7100–7107, 2011.

[21] P. Poizot, S. Laruelle, S. Grugeon, L. Dupont, and J.-M. Tarascon, "Nano-sized transition-metal oxides as negative-electrode materials for lithium-ion batteries," *Nature*, vol. 407, no. 6803, pp. 496–499, 2000.

[22] T.-J. Kim, D. Son, J. Cho, B. Park, and H. Yang, "Enhanced electrochemical properties of SnO_2 anode by $AlPO_4$ coating," *Electrochimica Acta*, vol. 49, no. 25, pp. 4405–4410, 2004.

[23] Y.-K. Sun, S.-W. Cho, S.-W. Lee, C. S. Yoon, and K. Amine, "AlF3-coating to improve high voltage cycling performance of $Li[Ni_{1/3}Co_{1/3}Mn_{1/3}]O_2$ cathode materials for lithium secondary batteries," *Journal of the Electrochemical Society*, vol. 154, no. 3, pp. A168–A172, 2007.

[24] D. Liu, Z. He, and X. Liu, "Increased cycling stability of $AlPO_4$-coated $LiMn_2O_4$ for lithium ion batteries," *Materials Letters*, vol. 61, no. 25, pp. 4703–4706, 2007.

[25] H. Shi, J. Barker, M. Y. Saïdi, and R. Koksbang, "Structure and lithium intercalation properties of synthetic and natural graphite," *Journal of the Electrochemical Society*, vol. 143, no. 11, pp. 3466–3472, 1996.

[26] T. Theivasanthi and M. Alagar, "X-ray diffraction studies of copper nanopowder," *Archives of Physics Research*, vol. 1, pp. 112–117, 2010.

[27] C.-H. Doh, H.-M. Shin, D.-H. Kim et al., "Improved anode performance of thermally treated SiO/C composite with an organic solution mixture," *Electrochemistry Communications*, vol. 10, no. 2, pp. 233–237, 2008.

[28] Z. H. Lu and J. R. Dahn, "Understanding the anomalous capacity of Li / Li [$Ni_xLi_{(1/3-2x/3)}Mn_{(2/3-x/3)}$] O_2 cells using *in situ* x-ray diffraction and electrochemical studies," *Journal of the Electrochemical Society*, vol. 149, pp. A815–A822, 2002.

[29] C. P. Grey, W.-S. Yoon, J. Reed, and G. Ceder, "Electrochemical activity of Li in the transition-metal sites of O_3 $Li[Li_{(1-2x)/3}Mn_{(2-x)/3}Ni_x]O_2$," *Electrochemical and Solid-State Letters*, vol. 7, no. 9, pp. A290–A293, 2004.

[30] J. R. Mueller-Neuhaus, R. A. Dunlap, and J. R. Dahn, "Understanding irreversible capacity in $Li_xNi_{1-y}Fe_{1-y}O_2$ cathode materials," *Journal of the Electrochemical Society*, vol. 147, no. 10, pp. 3598–3605, 2000.

[31] W. Luo, X. Hu, Y. Sun, and Y. Huang, "Electrospinning of carbon-coated MoO_2 nanofibers with enhanced lithium-storage properties," *Physical Chemistry Chemical Physics*, vol. 13, pp. 16735–16740, 2011.

[32] J. R. Dahn and W. R. McKinnon, "Structure and electrochemistry of $LixMoO_2$," *Solid State Ionics*, vol. 23, no. 1-2, pp. 1–7, 1987.

[33] Y. Liang, J. Sun, S. Yang, Z. Yi, and Y. Zhou, "Preparation, characterization and lithium-intercalation performance of different morphological molybdenum dioxide," *Materials Chemistry and Physics*, vol. 93, pp. 395–398, 2005.

[34] B.-C. Park, H.-B. Kim, S.-T. Myung et al., "Improvement of structural and electrochemical properties of AlF_3-coated

$Li[Ni_{1/3}Co_{1/3}Mn_{1/3}]O_2$ cathode materials on high voltage region," *Journal of Power Sources*, vol. 178, no. 2, pp. 826–831, 2008.

[35] G. Singh, R. Thomas, A. Kumar, R. S. Katiyar, and A. Manivannan, "Electrochemical and structural investigations on ZnO treated 0.5 Li_2MnO_3-0.5$LiMn_{0.5}Ni_{0.5}O_2$ layered composite cathode material for lithium ion battery," *Journal of the Electrochemical Society*, vol. 159, no. 4, pp. A470–A478, 2012.

[36] A. R. Armstrong, M. Holzapfel, P. Novák, M. Thackeray, and P. Bruce, "Demonstrating oxygen loss and associated structural reorganization in the lithium battery cathode $Li[Ni_{0.2}Li_{0.2}Mn_{0.6}]O_6$," *Journal of the American Chemical Society*, vol. 128, pp. 8694–88698, 2006.

[37] G. Li, Z. Yang, and W. Yang, "Effect of $FePO_4$ coating on electrochemical and safety performance of $LiCoCO_2$ as cathode material for Li-ion batteries," *Journal of Power Sources*, vol. 183, no. 2, pp. 741–748, 2008.

[38] B. V. Ratnakumar, M. C. Smart, and S. Surampudi, "Electrochemical impedance spectroscopy and its applications to lithium ion cells," *ChemInform*, vol. 33, p. 229, 2009.

[39] M. D. Levi, D. Aurbach, G. Salitra et al., "Solid-state electrochemical kinetics of Li-ion intercalation into $Li_{1-x}CoO_2$: simultaneous application of electroanalytical techniques SSCV, PITT, and EIS," *Journal of the Electrochemical Society*, vol. 146, no. 4, pp. 1279–1289, 1999.

[40] G. Ning, B. Haran, and B. N. Popov, "Capacity fade study of lithium-ion batteries cycled at high discharge rates," *Journal of Power Sources*, vol. 117, no. 1-2, pp. 160–169, 2003.

[41] J. Liu and A. Manthiram, "Understanding the improvement in the electrochemical properties of surface modified 5 V $LiMn_{1.42}Ni_{0.42}Co_{0.16}O_4$ spinel cathodes in lithium-ion cells," *Chemistry of Materials*, vol. 21, pp. 1695–1707, 2009.

[42] S. Sivaprakash and S. B. Majumder, "Spectroscopic analyses of 0.5$Li[Ni_{0.8}Co_{0.15}Zr_{0.05}]O_2-0.5Li[Li_{1/3}Mn_{2/3}]O_2$ composite cathodes for lithium rechargeable batteries," *Solid State Ionics*, vol. 181, no. 15-16, pp. 730–739, 2010.

[43] A. Chen, C. Li, R. Tang, L. Yin, and Y. Qi, "MoO_2-ordered mesoporous carbon hybrids as anode materials with highly improved rate capability and reversible capacity for lithium-ion battery," *Physical Chemistry Chemical Physics*, vol. 15, pp. 13601–13610, 2013.

[44] M. C. Smart, B. L. Lucht, and B. V. Ratnakumar, "Electrochemical characteristics of MCMB and LiNix Co_{1-x} O_2 electrodes in electrolytes with stabilizing additives," *Journal of the Electrochemical Society*, vol. 155, no. 8, pp. A557–A568, 2008.